Electronic Supplementary Material (ESI) for Physical Chemistry Chemical Physics

The impact of spectator species on the interaction of H_2O_2 with platinum – implications for the oxygen reduction reaction pathways

Ioannis Katsounaros, Wolfgang B. Schneider, Josef C. Meier, Udo Benedikt, P. Ulrich Biedermann, Angel Cuesta, Alexander A. Auer, and Karl J.J. Mayrhofer

(katsounaros@mpie.de; mayrhofer@mpie.de)

Supporting Information

1. Concentration decay in chloride-containing solution

Figure S1 shows the concentration of H_2O_2 vs. time (open circles) in an electrolysis experiment performed at +0.75 V_{RHE} in a 0.1 M $HClO_4$ + 1 10^{-3} M NaCl + 2 10^{-3} M H_2O_2 solution. The methodology followed in this experiment was described previously.[1] The solid curve shows the expected concentration decay assuming a mass-transport-limited transfer of two electrons, following Levich and Faraday equations (see ref. [1] for more details). We previously[1] showed that in a chloride-"free" 0.1 M $HClO_4$ solution, the theoretical prediction and the experimental data coincide at any potential between +0.2 V_{RHE} and +1.5 V_{RHE}, which led to the conclusion that the total rate of H_2O_2 decomposition (reduction rate + oxidation rate) is limited by the transport of H_2O_2. The observed deviation between the experimental data and the expected decay upon addition of chloride ions in the electrolyte, as shown in Figure S1, highlights the inhibition of hydrogen peroxide reduction due to the chloride adsorption at this potential.

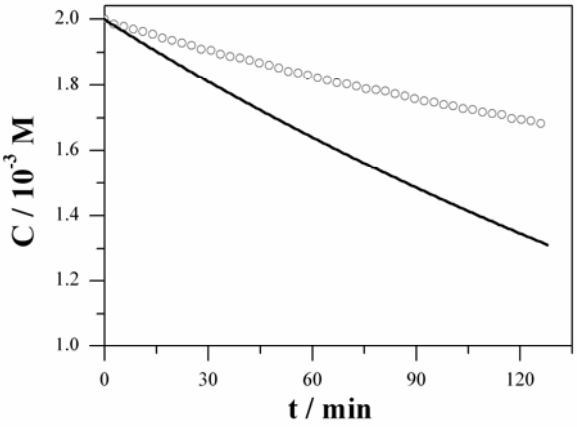

Figure S1. Concentration of hydrogen peroxide vs. time, during the electrolysis in 0.1 M $HClO_4$ + 1 10^{-3} M NaCl + 2 10^{-3} M H_2O_2 electrolyte at +0.75 V_{RHE}. The solid curve represents the expected concentration decay for a 2-electron diffusion-limited decomposition reaction. The methodology for this experiment has been described elsewhere.[1]

2. Voltammograms in iodide-containing solution

Figure S2 shows the positive direction of the background-corrected hydrodynamic voltammograms for (a) ORR and (b) PROR, in 0.1 M $HClO_4$ in which 1 10^{-4} M of different halide was added (see figure legend). The voltammograms for Cl^- and Br^- are described in the paper; the voltammogram for F^- (shown in Fig. 3 of the paper) is omitted from Fig. S2 for simplicity. The

addition of iodide in the $HClO_4$ solution suppresses ORR over a wide range of potentials, and ORR commences only below +0.4 V_{RHE}. Hydrogen peroxide reduction is even more strongly suppressed by the adsorption of iodide, and no reduction current is observable in the oxygen-free H_2O_2-containing solution in the potential region studied.

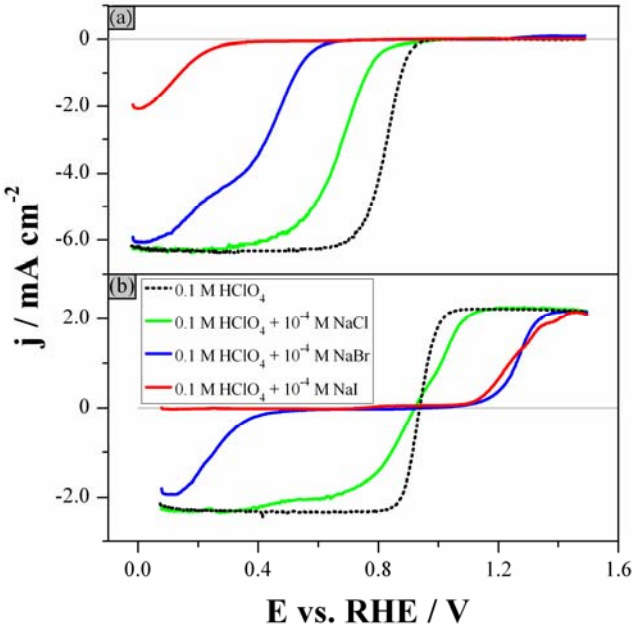

Figure S2. Hydrodynamic voltammograms in 0.1 M $HClO_4$ electrolyte, containing 1 10^{-4} M NaX where X: Cl^-, Br^- or I^- (see figure legend): (a) O_2-purged electrolyte and (b) Ar-purged electrolyte containing 1 10^{-3} M H_2O_2. Rotation rate: 1600 rpm. Scan rate: 0.1 V s^{-1}. Only the background-corrected positive-going sweep is shown.

3. Electronic structure calculations

3.1 Computational details

The calculations were carried out using the Orca program package.[2] The RI-BP86/Def2-TZVP level of theory was applied,[3–5] using the Stuttgart-pseudo potential for platinum including 60 electrons.[6,7] Convergence criteria were 10^{-7} a.u. for the energies and 10^{-4} a.u. in the gradient for geometries.

To model a Pt(111) surface, the bottom plane of a Pt_{37} cluster in hemispherical shape and a Pt-Pt distance of 2.78 Å was used.[8] Former investigations showed that small clusters with at least three layers of Pt and a diameter of approx. 1 Å yield results sufficiently close to those of slab calculations.[9,10] Furthermore, a ring of 12 water molecules was placed over the Pt atoms on the perimeter of the bottom plane to minimize the influence of edges as adsorption sites and to model the local environment of a water-covered surface.

3.2 Surface models and reference energies

To simulate various surface concentrations, two and three chlorine atoms were adsorbed over the remaining seven platinum atoms of the plane and a geometry optimization was carried out to obtain the structures as shown in Fig. S3 (for energies see Table S1). During the optimizations no constrains were applied to the positions of the seven central platinum atoms of the <111> plane and the chlorine atoms, while the other platinum atoms of the cluster and the water molecules

were kept fixed in their position. H_2O_2 or O_2 was adsorbed on the resulting geometries and optimized to the most stable surface configuration. To obtain potential energy profiles and transition states, constraint geometry optimizations were carried out for different O-O distances of H_2O_2 and O_2.

As the platinum cluster is an open-shell system, the potential energy surface scans were carried out for different spin states and the spin state with the lowest energy was chosen for each distance (see Tables S1 and S3). In order to calculate relative energies to the gas phase, reference energies were calculated for O_2 and H_2O_2, see Table S2. Solvation energies were estimated by calculations using the COSMO solvation model.[11] All energies were obtained with a constant charge, neglecting the influence of the adsorbed species on the Fermi energy and hence, the change of the electrochemical potential of the cluster. Currently, new schemes are being derived to go beyond this approximation.[12]

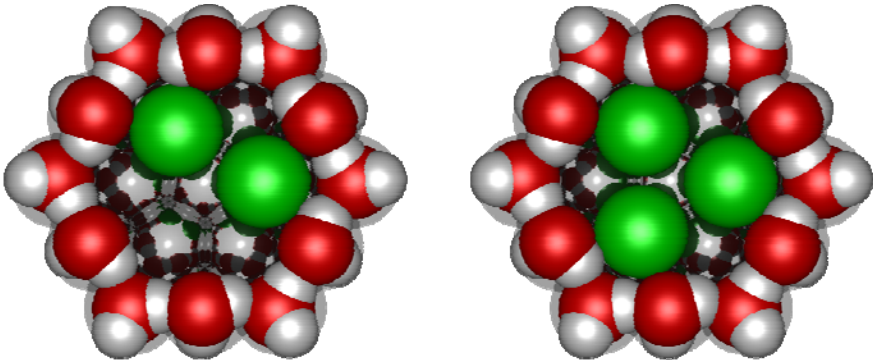

Figure S3. The surface models with two (left) and three (right) adsorbed chlorine atoms, shown with the van der Waals radii to illustrate the space available for the further adsorption of species.

Table S1. Absolute energies and spin states of the surface models with none, two or three adsorbed chlorine atoms

Number of adsorbed Cl atoms	Energy in a.u.	Spin
0	-5340.6992	5
2	-6261.2498	3
3	-6721.5221	3.5

Table S2. Absolute energies and spin states of H_2O_2 and O_2 in the gas phase and in the COSMO solvation model

Molecule	Energy in a.u.	Spin
H_2O_2	-151.6289	0
H_2O_2 (COSMO)	-151.6417	0
O_2	-150.4039	1
O_2 (COSMO)	-150.4042	1

3.3 H_2O_2 and O_2 dissociation

Table S3 shows detailed information on the calculations for the barriers for H_2O_2 and O_2 dissociation. The configurations listed in the table, correspond to those shown in Fig. 4 and 5 of the paper. In particular, the configurations 4b (Fig. S4) and 4c (Fig. S5) illustrate the H_2O_2 dissociation on the surface model including two and three chlorine atoms, respectively. The configurations 5a (Fig. S6) and 5b (Fig. S7) correspond to the O_2 dissociation on the surface model including no and two adsorbed chlorine atoms, respectively. The values for the dissociation of H_2O_2 at the bare surface can be found in Katsounaros et al.[1]

Table S3. Absolute energies, O-O distances and the spin state of the structures involved in the dissociation of H_2O_2 and O_2 on the surface models. The values for the energy E_{rel} are relative to the energy of H_2O_2 in the gas phase (see Table S2).

Geometry		Energy in a.u.	O-O distance in Å	Spin	E_{rel} in eV
Configuration 4b	Adsorbed H_2O_2	-6412.8922	1.46	5	-0.37
	Transition State	-6412.8870	1.60	5	-0.23
	Local Minimum	-6412.9273	2.72	4	-1.32
	Final configuration	-6412.9438	2.67	4	-1.77
Configuration 4c	Adsorbed H_2O_2	-6873.1063	1.47	3.5	1.22
	Transition State	-6873.1045	1.60	3.5	1.27
	Final configuration	-6873.1521	2.71	3.5	-0.03
Configuration 5a	Adsorbed O_2	-5491.1106	1.31	7	-0.20
	Transition State	-5491.0840	2.00	7	0.52
	Final configuration	-5491.1299	2.86	7	-0.73
Configuration 5b	Adsorbed O_2	-6411.6587	1.31	5	-0.14
	Final configuration	-6411.6214	2.50	7	0.88

For the dissociation of H_2O_2 on the surface model with two co-adsorbed chlorine, the barrier was found to be approx. 0.1 eV lower than on the bare surface. The difference can be explained by the hydrogen bonds to the chlorine atoms that stabilize the transition state.

The dissociation of H_2O_2 proceeds by cleaving the O-O bond, while two OH···Cl hydrogen bonds are maintained, yielding a local minimum. A further reduction of the energy by 0.45 eV is obtained by forming an OH···O hydrogen bond (see Fig. S4 and Table S3). The difference between the two minima allows estimating the energy difference between a Cl···H hydrogen bond and an O···H hydrogen bond at the surface.

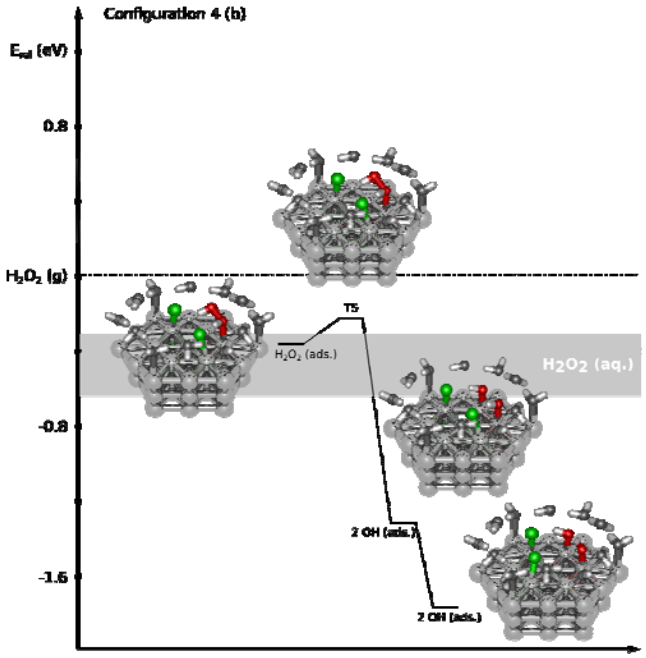

Figure S4. Energy profile for the dissociation of H_2O_2 for the surface model with two chlorine atoms (configuration 4b). The energies are given relative to H_2O_2 in the gas phase (dashed line). The gray bar indicates the range of estimates for the H_2O_2 solvation energies.

The surface model with three adsorbed chlorine atoms (figure S5 and table S3) is an extreme model, which was devised to investigate whether H_2O_2 will dissociate under extreme spatial restrictions of the local environment.

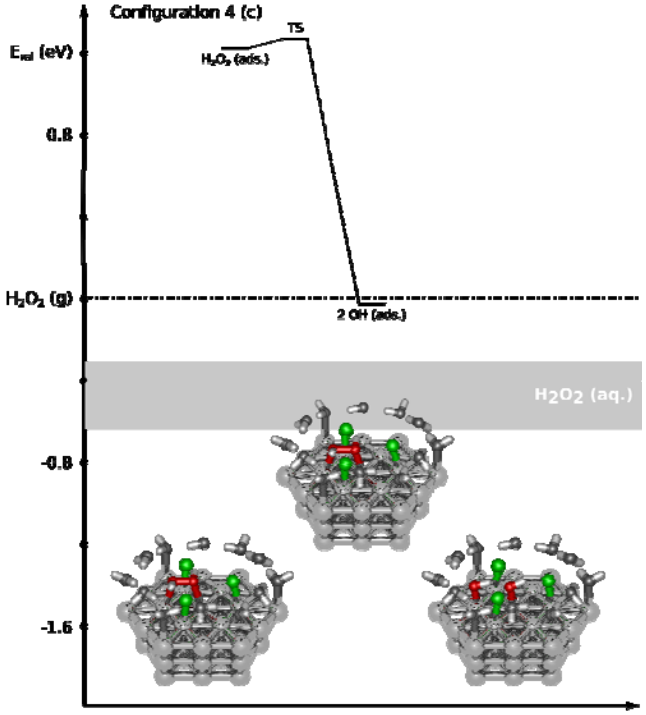

Figure S5. Energy profile for the dissociation of H_2O_2, for the surface model with three chlorine atoms (configuration 4c). The energies are given relative to H_2O_2 in the gas phase (dashed line). The gray bar corresponds to H_2O_2 in solution.

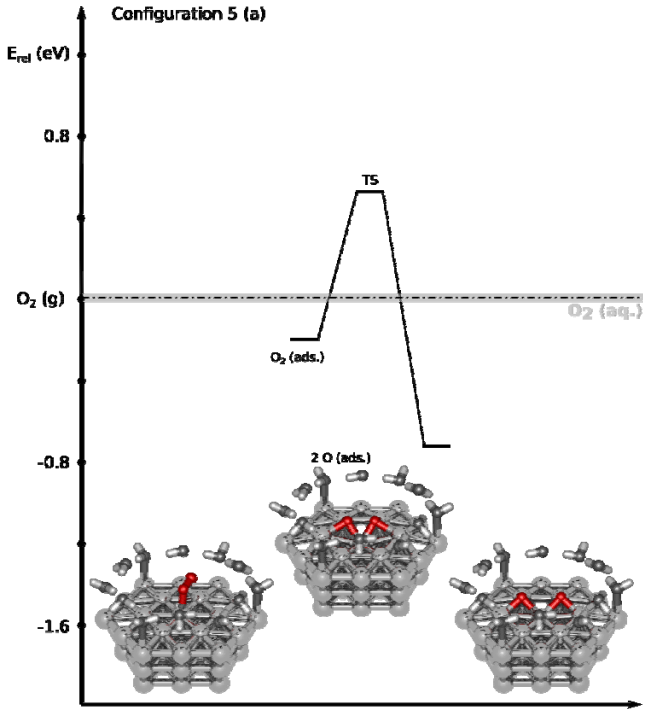

Figure S6: Energy profile for the dissociation of O_2 for the surface model for the bare surface (configuration 5a). The energies are given relative to O_2 in the gas phase (dashed line).

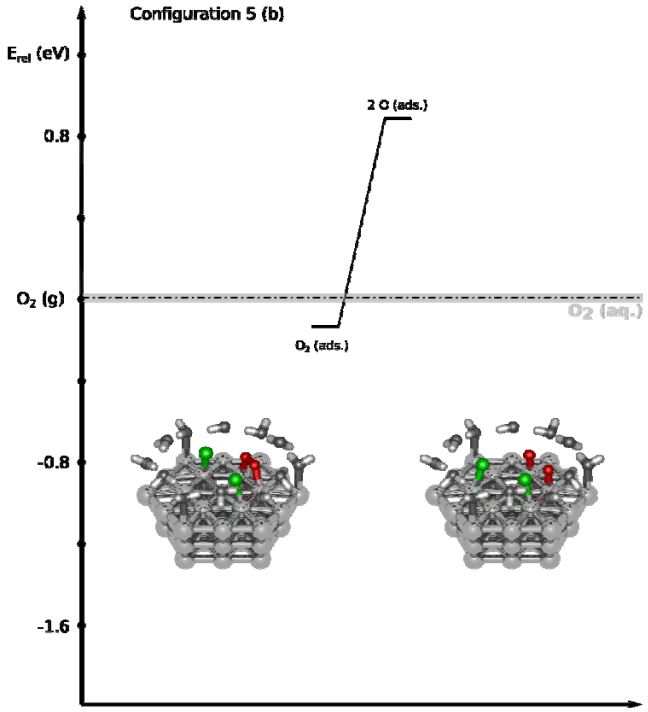

Figure S7. Energy profile for the dissociation of O_2 for the surface model for the bare surface (configuration 5b). The energies are given relative to O_2 in the gas phase (dashed line).

References

1. I. Katsounaros, W. B. Schneider, J. C. Meier, U. Benedikt, P. U. Biedermann, A. A. Auer, and K. J. J. Mayrhofer, *Phys. Chem. Chem. Phys.*, 2012, **14**, 7384–7391.
2. F. Neese, *WIREs Comput. Mol. Sci.*, 2012, **2**, 73–78.

3. F. Weigend and R. Ahlrichs, *Phys. Chem. Chem. Phys.*, 2005, **7**, 3297–3305.
4. J. P. Perdew, *Phys. Rev. B*, 1986, **33**, 8822–8824.
5. A. D. Becke, *Phys. Rev. A*, 1988, **38**, 3098–3100.
6. D. Andrae, U. Haussermann, M. Dolg, H. Stoll, and H. Preuss, *Theor. Chim. Acta*, 1990, **77**, 123–141.
7. F. Weigend, *Phys. Chem. Chem. Phys.*, 2006, **8**, 1057–1065.
8. L. Wang, A. Roudgar, and M. Eikerling, *J. Phys. Chem. C*, 2009, **113**, 17989–17996.
9. T. Jacob and W. A. Goddard, *ChemPhysChem*, 2006, **7**, 992–1005.
10. M. Kettner, W. B. Schneider, and A. A. Auer, *J. Phys. Chem. C*, 2012, **116**, 15432–15438.
11. A. Klamt and G. Schüürmann, *J. Chem. Soc. Perkin Trans.*, 1993, 799–805.
12. U. Benedikt, W. B. Schneider, and A. A. Auer, *Phys. Chem. Chem. Phys.*, 2013, **15**, 2712–2724.